

CMB lensing in a modified Λ CDM model in light of the H_0 tension

Hossein Moshafi^{1,*}, Shant Baghrām^{2,†} and Nima Khosravi^{3,4,‡}

¹*School of Astronomy, Institute for Research in Fundamental Sciences (IPM),
P.O. Box 19395-5531 Tehran, Iran*

²*Department of Physics, Sharif University of Technology, P.O. Box 11155-9161 Tehran, Iran*

³*Department of Physics, Shahid Beheshti University, 1983969411 Tehran, Iran*

⁴*School of Physics, Institute for Research in Fundamental Sciences (IPM),
P.O. Box 19395-5531 Tehran, Iran*



(Received 7 January 2021; accepted 5 August 2021; published 2 September 2021)

The observed discrepancy of the Hubble parameter measurements in the local universe with the cosmic microwave background (CMB) data may indicate a new physics. It is vital to test the alternative models that reconcile the Hubble tension with other cosmological observations in this direction. The CMB lensing is a crucial observation that relates the early universe perturbations to the matter's late-time distribution. In this work, we study the prediction of the $\ddot{u}\Lambda$ CDM as a solution for H_0 tension for CMB lensing and the low- and high- ℓ 's temperature (TT) power spectrum internal inconsistency. We show that this model relaxes the low- and high- ℓ 's TT mild inconsistency and the CMB lensing tensions simultaneously. Accordingly, $\ddot{u}\Lambda$ CDM having the same number of free parameters as Λ CDM with lensing amplitude A_L added, has a better fit with $\Delta\chi^2 = -3.3$.

DOI: [10.1103/PhysRevD.104.063506](https://doi.org/10.1103/PhysRevD.104.063506)

I. INTRODUCTION

The recent observations of local standard candles, which leads to a more precise measurement of the cosmos' expansion rate and determination of the Hubble constant H_0 , introduce a new challenge to cosmology's standard paradigm. The challenge is the apparent discrepancy of the local measurements of H_0 [1–3] with the value obtained from cosmic microwave background (CMB) observations [4]. There are some other anomalies between local datasets and CMB if the standard model of cosmology Λ CDM is assumed. One of the famous ones is the amount of matter content σ_8 measured locally [5] in comparison to CMB [4]. Besides, an internal inconsistency is reported in Planck results [4] in measurements of CMB lensing amplitude, A_L , which can be related to low/high- ℓ inconsistency. These issues, if not systematic errors, trigger many interests in cosmological model building.

The idea that a new physics is needed to explain this discrepancy (H_0 tension) opens a vast arena for model building and phenomenological predictions. The ideas span a vast range starting from dark sector interactions [6–22], early dark energy models which modify sound horizon [23–25], phase transition in dark energy [26–31] to the modified gravity models [32–34]. The Hubble constant tension, on the one hand, and the proposed models to

solve this tension, on the other hand, remind us that the unknown nature of dark matter and dark energy is at the heart of the problem. In this direction, the long-standing question of cosmological constant and plausible gravity models leads to a class of solutions known as ensemble theories of gravity [35,36]. This idea proposes a density-dependent transition of the law of gravity. In this direction a cosmological model is introduced known as $\ddot{u}\Lambda$ CDM in [37]. We showed $\ddot{u}\Lambda$ CDM can address H_0 tension.

In this work, we want to check if $\ddot{u}\Lambda$ CDM can address the CMB lensing inconsistency in addition to the Hubble tension. While having local H_0 measurements allows us to check the background of our model, the CMB lensing checks $\ddot{u}\Lambda$ CDM at the level of its perturbations. Another reason for this choice is that the lensing in cosmological scales from the CMB to late-time lenses such as cosmic shear observations are promising tools to detect the deviations from the standard model of cosmology [38,39]. We also study the effect of the integrated Sachs-Wolfe (ISW) in this context. The ISW is related to the change of potential from the last scattering to the observer, and it is the other gravitational secondary effect on the CMB besides the lensing effect.

The structure of this work is as follows: In Sec. II, we review the ensemble theory of gravity and the $\ddot{u}\Lambda$ CDM model. In Sec. III, we study the lensing and ISW of the $\ddot{u}\Lambda$ CDM. In Sec. IV, we discuss the data and methodology. In Sec. V, we show the results, and in Sec. VI, we conclude, and we have our future remarks.

*moshafi@ipm.ir

†baghrām@sharif.edu

‡n-khosravi@sbu.ac.ir

II. ENSEMBLE AVERAGE THEORY OF GRAVITY TO $\ddot{u}\Lambda$ CDM

The ensemble average theory of gravity [35,36] suggests that the gravity model works in the Universe are an ensemble average of theoretically possible models of gravity. This idea is formulated in the Lagrangian formalism via the relation below:

$$\mathcal{L} = \left(\sum_{i=1}^N \mathcal{L}_i e^{-\beta \mathcal{L}_i} \right) / \sum_{i=1}^N e^{-\beta \mathcal{L}_i}, \quad (1)$$

where \mathcal{L}_i are theoretically possible Lagrangians and β is a free parameter of the model. A possible and simple derivation of a model from the ensemble theory idea is the \ddot{u} -gravity gravity model which used the power law terms in the Ricci scalar as a plausible candidate of $f(R)$ gravity models which make an independent basis for model space such as

$$\mathcal{L}_{\ddot{u}ber} = \left(\sum_{i=1}^N (\bar{R}^n - 2\Lambda) e^{-\beta(\bar{R}^n - 2\Lambda)} \right) / \sum_{i=1}^N e^{-\beta(\bar{R}^n - 2\Lambda)}, \quad (2)$$

where $\bar{R} = R/R_0$; in this case R_0 is a free parameter of the model. We call it $\ddot{u}\Lambda$ CDM. This cosmological model is an extension of the standard model. This leads to a simple model for the gravity as [37]

$$\text{Gravity} \simeq \begin{cases} R = R_0 & \rho < \rho_{\ddot{u}} \\ \Lambda\text{CDM} & \rho > \rho_{\ddot{u}}, \end{cases} \quad (3)$$

where $\rho_{\ddot{u}}$ is the critical density in which the transition occurred. In the case, if the density is higher than the critical value which $\rho > \rho_{\ddot{u}}$ we recover the standard model with the cosmological constant and in the regime of $\rho < \rho_{\ddot{u}}$ we have constant Ricci scalar. The transition occurs in z_{\oplus} , where in two regimes the background evolution will be

$$E^2(z) = \Omega_m(1+z)^3 + \Omega_\Lambda, \quad z > z_{\oplus}, \quad (4)$$

where $E(z) = H/H_0$ is the normalized Hubble parameter:

$$E^2(z) = \frac{1}{2}\bar{R}_0 + \left(1 - \frac{1}{2}\bar{R}_0\right)(1+z)^4, \quad z < z_{\oplus}, \quad (5)$$

where $\bar{R}_0 = R_0/6H_0^2$. The continuity condition for $E(z)$ and dE/dz imposes that we have only one more free parameter z_{\oplus} in comparison to Λ CDM.

In order to study the perturbation theory, the $\ddot{u}\Lambda$ CDM behavior is exactly derived from the action below:

$$S = \frac{1}{16\pi G} \int d^4x \sqrt{-g} [\xi(R - R_0) - \lambda] + \mathcal{L}_m, \quad (6)$$

where g is the determinant of the metric $g_{\mu\nu}$, and R_0 is a constant free parameter of the model. ξ is the Lagrange multiplier, which ensures that after the transition redshift the Ricci scalar is constant and it is equal to $R = R_0$. For $z > z_{\oplus}$, we want to recover the standard Λ CDM model, so in this era $\xi = 1$ and $\lambda = 2\Lambda - R_0$, where Λ is the cosmological constant in the Λ CDM. Accordingly, this action will give us the equation of the motion and the trace of the field equation governing the dynamics of the field ξ :

$$\xi R_0 = 8\pi G T - 2\lambda - 3\square\xi, \quad (7)$$

where $T = g_{\mu\nu} T^{\mu\nu}$ is the trace of energy-momentum tensor. Now we can use the above Lagrangian to study the perturbation theory of our model after the transition in $\ddot{u}\Lambda$ CDM, i.e., $z < z_{\oplus}$. We define the Bardeen gravitational potentials $\Psi(\vec{x}, \eta)$ and $\Phi(\vec{x}, \eta)$ in the perturbed Friedmann-Robertson-Walker metric as

$$ds^2 = a^2(\eta) [-(1 + 2\Psi(\vec{x}, \eta))d\eta^2 + (1 - 2\Phi(\vec{x}, \eta))d\chi^2], \quad (8)$$

where η is the conformal time. Now we perturb the quantities in the theory as below up to first order (with superscript 1 for ξ):

$$R = R_0, \quad (9)$$

$$\xi = \xi^0(\eta) + \xi^1(\vec{x}, \eta), \quad (10)$$

$$T_{\mu\nu} = \bar{T}_{\mu\nu}(\eta) + \delta T_{\mu\nu}(\vec{x}, \eta), \quad (11)$$

$$T = \bar{T}(\eta) + \delta T(\vec{x}, \eta). \quad (12)$$

The background equations of motion are

$$\frac{R_0 a^2}{3} = 2 \frac{a''}{a}, \quad (13)$$

$$\frac{R_0 a^2}{3} = \frac{8\pi G \bar{T} a^2}{3\xi^0} + 2\mathcal{H} \frac{\xi^{0'}}{\xi^0} + \frac{\xi^{0''}}{\xi^0} - \frac{2}{3} a^2 \lambda, \quad (14)$$

$$\frac{R_0 a^2}{3} = \frac{16\pi G \bar{T}_0^0 a^2}{3\xi^0} + 2\mathcal{H} \left(\mathcal{H} + \frac{\xi^{0'}}{\xi^0} \right) - \frac{\lambda a^2}{3\xi^{(0)}}, \quad (15)$$

where $\mathcal{H} = a'/a$ and $'$ is the derivative with respect to conformal time η .

The equations of motion at linear order are

$$\nabla^2(\Psi - 2\Phi) = -\Psi R_0 a^2 - 3\mathcal{H}(3\Phi' + \Psi') - 3\Phi'', \quad (16)$$

$$\begin{aligned} \frac{R_0 a^2}{3} \xi^1 &= \frac{8\pi G a^2}{3} \delta T - 2\mathcal{H}(2\Psi \xi^{0'} - \xi^{1'}) - \square \xi^1 \\ &\quad - \xi^{0'}(3\Phi' + \Psi') - 2\Phi \xi^{0''}, \end{aligned} \quad (17)$$

$$\begin{aligned} \frac{R_0 a^2}{3} \xi^1 &= \frac{16\pi G a^2}{3} \delta T_0^0 + 3\xi^1 \mathcal{H}^2 + \frac{4}{3} \xi^0 \nabla^2 \Phi \\ &- \mathcal{H}(\mathcal{H}\Psi + \Phi') - 2\mathcal{H}(2\Phi \xi^{0'} - \xi^{1'}) - \frac{2}{3} \nabla^2 \xi^1. \end{aligned} \quad (18)$$

The $\{0i\}$ component of the equation of motion is

$$2\xi^0(\mathcal{H}\Psi_{,i} + \Phi'_{,i}) = 8\pi G \delta T_{0i} - \mathcal{H}\xi^1_{,i} - \Psi_{,i}\xi^{0'} + \xi^{1'}_{,i}. \quad (19)$$

Using the equation of motions in the linear scalar perturbation we can write the Newtonian potential Ψ and lensing potential ϕ_L in the quasistatic regime ($\nabla^2 \gg \mathcal{H}^2$) [37]:

$$\begin{aligned} \nabla^2 \Psi &= \frac{16\pi G a^2}{3\xi(z)} \delta\rho, \\ \phi_L &= \frac{\Phi + \Psi}{2} = \frac{3}{4} \Psi. \end{aligned} \quad (20)$$

The continuity, Euler equation and the evolution of dark matter density contrast (growth function) are given accordingly:

$$\delta' = -\theta + 3\Phi' \quad (21)$$

$$\theta' + \mathcal{H} = -\nabla^2 \Psi \quad (22)$$

$$\delta'' + \mathcal{H}\delta' - \frac{16\pi G a^{-1}}{3\xi^0(\eta)} \bar{\rho}\delta = 0. \quad (23)$$

It is worth mentioning that we modify the Poisson equation by replacing $8\pi G \rightarrow 16\pi G/(3\xi(z))$ after the transition. On the other hand, we have $\Phi = \Psi$ in general relativity which is not always the case in modified gravity models [40]. It is the case in our model, and we change the gravitational lensing potential by replacing the $\phi_L = \Psi \rightarrow \phi_L = 3\Psi/4$ after the transition. However, an important point to note here is that the lensing potential is continuous in transition redshift. This is because the Ψ is $4/3$ times the Λ CDM model. This is a crucial point, which enables us to calculate the ISW effect in the upcoming section. Note that for $z > z_\oplus$ we use the standard perturbation theory for the Λ CDM model and match them to the ones coming from $\ddot{u}\Lambda$ CDM (20) at $z = z_\oplus$ and $z < z_\oplus$; we use the $\ddot{u}\Lambda$ CDM perturbation theory.

III. PLANCK INTERNAL (IN)CONSISTENCIES IN $\ddot{u}\Lambda$ CDM

In [4], they check the internal consistency of the CMB dataset. In this direction, they report two (mild) inconsistencies: the low- and high- ℓ 's temperature (TT) power spectrum are in $\sim 2\sigma$ tension and the amplitude of lensing A_L is higher than unity again around 2σ . In this section, we are studying these two (in)consistencies in the context of

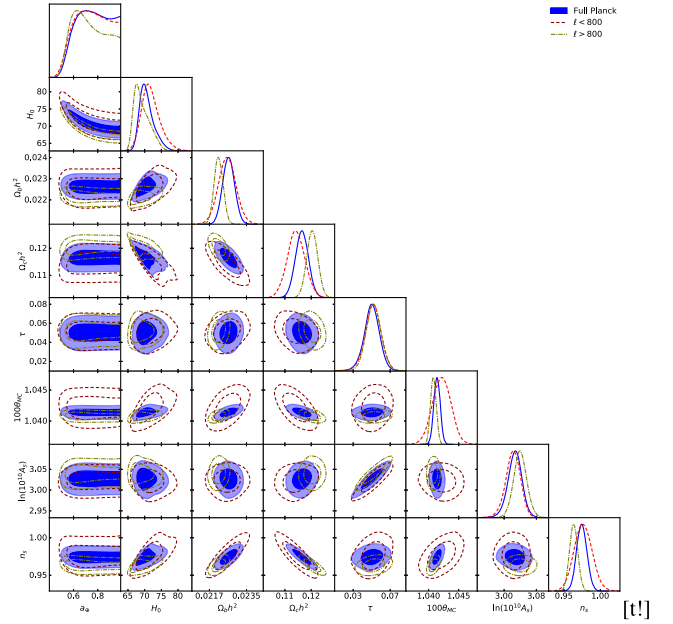


FIG. 1. The contour plot of $\ddot{u}\Lambda$ CDM parameters is represented for high- ℓ 's with green dash-dotted lines and low- ℓ 's with red dashed lines. The blue contour plots show the 1σ and 2σ constraints with full Planck TT data.

$\ddot{u}\Lambda$ CDM. We check our results against the higher H_0 value reported by Riess *et al.* [3] to see if $\ddot{u}\Lambda$ CDM can address internal inconsistencies and H_0 tension simultaneously. We also check ISW in our model with galaxy cross-correlation. The ISW effect is also related to the change of the gravitational potential.

A. Low- and high- ℓ 's

We check our model against the low- and high- ℓ TT power spectrum separately and we show the results in Fig. 1 and Table I. The contour plots show no inconsistencies between low- and high- ℓ 's in the $\ddot{u}\Lambda$ CDM framework. This result allows us to add them up together and use the full CMB TT power spectrum in our upcoming analysis.

B. Lensing in $\ddot{u}\Lambda$ CDM

In this section, we will study the CMB lensing in the context of $\ddot{u}\Lambda$ CDM. Due to Eq. (20), the lensing potential in $\ddot{u}\Lambda$ CDM named as $\phi^{\ddot{u}}$ is as

$$\phi^{\ddot{u}}(\hat{n}) = -2 \int_0^{\chi_*} d\chi \left(\frac{\chi_* - \chi}{\chi_* \chi} \right) \phi_L, \quad (24)$$

where \hat{n} is direction of the observation, and χ_* is the comoving distance to the last scattering. Note that in the standard Λ CDM case $\phi_L = \Psi$ and Ψ are obtained from the standard Poisson equation $\nabla^2 \Psi = 4\pi G a^2 \delta\rho$ [41]. The angular power spectrum of the lensing is obtained as

TABLE I. 68% C.L. constraints for the $\ddot{\Lambda}$ CDM, for Planck data in two ranges $\ell < 800$ and $\ell > 800$.

Parameters	Planck	
	$2 < \ell < 800$	$800 < \ell < 2500$
$\Omega_b h^2$	0.02256 ± 0.00043	0.02215 ± 0.00022
$\Omega_c h^2$	0.1143 ± 0.0034	0.1204 ± 0.0021
Ω_m	0.268 ± 0.025	$0.300^{+0.026}_{-0.019}$
H_0	$71.9^{+2.1}_{-3.1}$	$69.2^{+1.5}_{-2.9}$
a_\oplus	0.75 ± 0.13	$0.73^{+0.11}_{-0.18}$
S_8	0.800 ± 0.049	0.888 ± 0.036
$100\theta_{MC}$	1.0422 ± 0.0015	1.04080 ± 0.00047
$\ln(10^{10} A_s)$	$3.022^{+0.019}_{-0.017}$	3.040 ± 0.017
n_s	0.9745 ± 0.0070	0.9633 ± 0.0057
τ	0.0515 ± 0.0089	0.0521 ± 0.0082

$$\ell^4 C_\ell^{\phi\phi} = 18\Omega_m^2 H_0^4 \int_0^{\chi_*} d\chi \chi^2 \left(\frac{\chi_* - \chi}{\chi_* \chi} \right)^2 P_m^{\ddot{\Lambda}} \left(\frac{\ell}{\chi} \right) \times \left[\frac{D^{\ddot{\Lambda}}(z)(1+z)}{D^{\ddot{\Lambda}}(z=0)\xi(z)} \right]^2, \quad (25)$$

where $P_m^{\ddot{\Lambda}}(\frac{\ell}{\chi})$ is the matter power spectrum of $\ddot{\Lambda}$ CDM in present time and $D^{\ddot{\Lambda}}(z)$ is the growth function of the model obtained from Eq. (23). We should note that the $\ddot{\Lambda}$ CDM power spectrum, growth function, and lensing potential are the same as the Λ CDM model for $z > z_\oplus$. This means that for $z > z_\oplus$ we have $\xi(z) \rightarrow 1$, $\Phi_L \rightarrow \Psi$, $D^{\ddot{\Lambda}}(z) \rightarrow D(z)$ and $P_m^{\ddot{\Lambda}} \rightarrow P_m$, where $D(z)$ and $P_m(z)$ are Λ CDM growth function and power spectrum. Accordingly, the integral in Eq. (25) is a sum of two integrals one from zero to comoving distance related to transition redshift ($0, \chi(z_\oplus)$) and then the other integral from $(\chi(z_\oplus), \chi_*)$. In first one we use the $\ddot{\Lambda}$ CDM lensing potential which leads to corresponding power spectrum and growth function and in the second part of the integral we have the Λ CDM lensing potential, integrated in line of sight. In Fig. 2, we plot the angular power spectrum of lensing for both standard model and $\ddot{\Lambda}$ CDM. The data points are from Planck 2018 [42], Polarbear 2019 and SPTpol2019 [43].

C. ISW in $\ddot{\Lambda}$ CDM

The integrated Sachs Wolfe (ISW) effect introduces secondary anisotropy on the CMB. ISW is the imprint of the dynamical gravitational potentials on the CMB photons. The ISW effect in $\ddot{\Lambda}$ CDM is as below:

$$\frac{\Delta T}{T} \Big|_{\text{ISW}} = 2 \int_0^{\chi_*} d\chi e^{-\tau} \frac{\partial \phi_L}{\partial \chi}, \quad (26)$$

where τ is the optical depth defined as the line of sight integral of number density of free electrons n_e as $\tau = \int_{\eta_i}^{\eta_0} n_e \sigma_T d\eta$. Note that for $z > z_\oplus$, similar to the

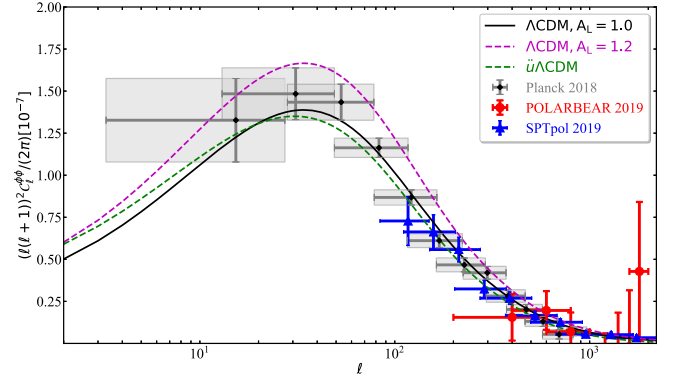


FIG. 2. The angular power spectrum of the CMB lensing is plotted for $\ddot{\Lambda}$ CDM, Λ CDM with and without free A_L . It is obvious that $\ddot{\Lambda}$ CDM mimics Λ CDM with $A_L = 1$ without any inconsistency with the data points. Note that the temperature power spectrum prefers Λ CDM with $A_L = 1.2$ which is not consistent with CMB lensing power spectrum.

CMB lensing case, we have $\Phi_L \rightarrow \Psi$. Due to the cosmic variance effect, it is hard to find the signal in CMB alone. Accordingly, the ISW effect is extracted via the cross-correlation with the galaxy distribution. The sophisticated idea is that the same potential which affects the CMB anisotropies is the same potential that governs the dynamics of the dark matter halos. Halos are the host of the galaxies. Accordingly, the ISW signal is extracted via the ISW-galaxy cross-correlation function or its angular power spectrum C_ℓ^{gT} as [44]

$$C_\ell^{gT} = \frac{2}{\pi} \int_0^\infty k^2 dk I_\ell^{\text{ISW}}(k) I_\ell^g(k) P_m^{\ddot{\Lambda}}(k), \quad (27)$$

where $P_m^{\ddot{\Lambda}}(k)$ is the matter power spectrum of $\ddot{\Lambda}$ CDM in the present time which must be transferred to the Λ CDM power spectrum in redshifts $z > z_\oplus$. Note that $I_\ell^{\text{ISW}}(k)$ and $I_\ell^g(k)$ are the kernels of ISW and galaxy distribution defined as

$$I_\ell^{\text{ISW}}(k) = \frac{3H_0^2 \Omega_m}{k^2} \int dz \frac{d}{dz} \left[\frac{D^{\ddot{\Lambda}}(z)(1+z)}{D^{\ddot{\Lambda}}(z=0)\xi(z)} \right] j_\ell(k\chi(z)), \quad (28)$$

$$I_\ell^g(k) = \int dz b(k, z) \frac{dN}{dz} \left[\frac{D^{\ddot{\Lambda}}(z)}{D^{\ddot{\Lambda}}(z=0)\xi(z)} \right] j_\ell(k\chi(z)), \quad (29)$$

where $\frac{dN}{dz}$ is the distribution function of galaxies in redshift, which is used in the cross-correlation procedure and is normalized to unity $\int dz \frac{dN}{dz} = 1$. Note that $b(k, z)$ is the bias parameter of galaxies distribution to dark matter halos and j_ℓ is the spherical Bessel function which depends on comoving distance and wave number. In this work, we assume that the bias parameter is unity. Note that

TABLE II. Flat priors on the cosmological parameters varied in this paper.

Parameter	Symbol	Prior
Cold dark matter density	$\Omega_c h^2$	[0.001, 0.99]
Baryon density	$\Omega_b h^2$	[0.005, 0.1]
Transition scale factor	a_{\oplus}	[0.4, 1.0]
Lensing amplitude	A_L	[0.5, 3.0]
Amplitude of scalar spectrum	$\ln(10^{10} A_s)$	[1.61, 3.91]
Scalar spectral index	n_s	[0.8, 1.2]
Angular scale at decoupling	$100\theta_{MC}$	[0.5, 10.0]
Optical depth	τ	[0.01, 0.8]
Pivot scale [Mpc^{-1}]	k_{pivot}	0.05

cosmology can change the bias parameter as well. This effect in ISW-galaxy cross-correlation is studied [45]. In this work, we assume that the bias is almost unchanged. It is worth mentioning again that, although the Poisson equation and the relation of the lensing potential to Ψ are changed in $\ddot{u}\Lambda$ CDM, the lensing potential is unchanged in transition redshift. In the next section, we present the methodology and observational data which we used in this study.

IV. METHODOLOGY AND OBSERVATIONAL DATA

In this section, we use a combination of recent early universe and late-time measurements to constrain the $\ddot{u}\Lambda$ CDM as follows:

- (i) *Cosmic microwave background*.—We consider the CMB temperature, polarization, and lensing reconstruction angular power spectra as measured by the 2018 Planck legacy release [4,46]. We denote “Planck,” which includes the CMB temperature and polarization data (TT, TE, EE + lowE; where the low-multipole polarization is obtained from the

high-frequency instrument, HFI), and also we denote “Planck + lensing” which additionally includes the lensing reconstruction (TT, TE, EE + lowE + lensing).

- (ii) *Hubble Space Telescope (HST)*.—We also use the recent estimation of the Hubble constant, $H_0 = 74.02 \pm 1.42$ at 68% confidence level (C.L.) obtained from the Hubble Space Telescope [3]. In this paper, we refer to this data as “R19.”
- (iii) *ISW-galaxy cross-correlation*.—For this observable we use NRAO VLA Sky Survey (NVSS) [47] and Wide-field Infrared Survey Explorer (WISE) dataset [48,49].

In our cosmological analysis, we perform Markov chain Monte Carlo (MCMC) calculations with a modified version of MGCosmoMC publicly available code [50] and standard public code CosmoMC [51]. We use a convergence criterion that obeys $R - 1 < 0.01$, where the Gelman-Rubin R -statistics [52] is the variance of chain means divided by the mean of chain variances.

We consider a seven parameters model with six of the Λ CDM model parameters plus lensing amplitude parameter A_L . Also, for the $\ddot{u}\Lambda$ CDM model we consider an extra parameter, transition scale factor ($a_{\oplus} = (1 + z_{\oplus})^{-1}$). Assumption for priors of parameters are listed in Table II. In the next section, we will discuss the observational constraints on the model’s free parameter based on lensing observations.

V. RESULTS: PARAMETER ESTIMATION

In this section we examine the standard model and $\ddot{u}\Lambda$ CDM, facing the CMB Planck data [4] and CMB lensing data [42] and also the H_0 measurements by Riess *et al.* [3]. In the left panel of Fig. 3, we plot the likelihood of the A_L parameter for the six parameter standard Λ CDM with CMB Planck data, which shows a

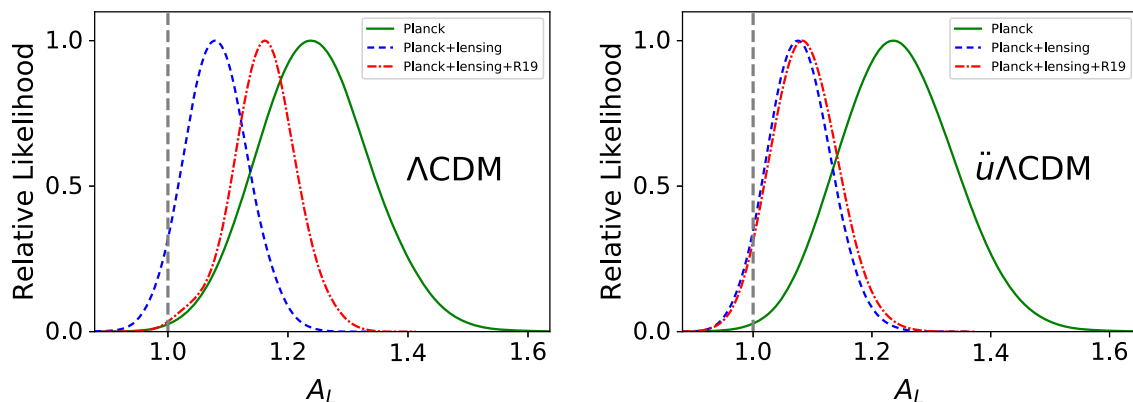


FIG. 3. The relative likelihood of the A_L parameter is plotted for the standard Λ CDM and $\ddot{u}\Lambda$ CDM models in left and right, respectively. Both models have ~ 2 – 3σ tension when we checked them against only the Planck dataset (green curves). When we add the lensing data (blue curves), both models are consistent with $A_L = 1$ in their 1σ regions. Adding R19 (red curves) restores the 2 – 3σ tension for the Λ CDM. CMB lensing and R19 datasets are not compatible in the Λ CDM. However $\ddot{u}\Lambda$ CDM shows no inconsistency between lensing and R19 datasets.

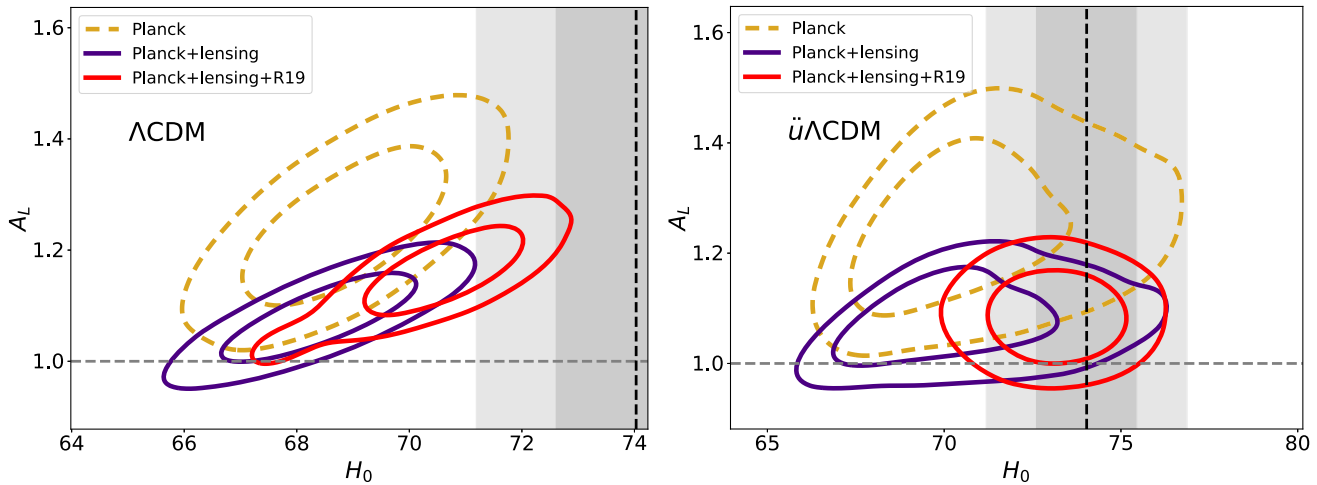


FIG. 4. We have plotted two-dimensional likelihood for A_L vs H_0 for Λ CDM and $\ddot{u}\Lambda$ CDM in the left and right, respectively. All the datasets' combinations of the Λ CDM model show a positive correlation between A_L and H_0 . That is why it is difficult for Λ CDM to be consistent for both $A_L = 1$ and R19 simultaneously. However, this correlation seems broken for the case of $\ddot{u}\Lambda$ CDM.

tension for the Lensing amplitude. Adding the free parameter A_L reconciles this tension. Interestingly adding the local SNeIa data worsens the situation. In contrast, the proposed $\ddot{u}\Lambda$ CDM is compatible with both CMB lensing and the R19 distance indicator result. In the right panel of Fig. 3, the red dash-dotted line shows the combination of Planck+lensing+R19 data for $\ddot{u}\Lambda$ CDM, which is almost compatible with $A_L \sim 1$. This means that the $\ddot{u}\Lambda$ CDM has the same number of parameters as the standard model with A_L .

In Fig. 4, we show the two-dimensional likelihood for A_L vs H_0 for Λ CDM and $\ddot{u}\Lambda$ CDM in the left and right panels, respectively. For all the datasets' combinations, the Λ CDM model shows a positive correlation between A_L and H_0 . That is why the Λ CDM cannot be consistent for both $A_L = 1$ and R19 simultaneously. However, this correlation seems broken for the case of $\ddot{u}\Lambda$ CDM. The modified gravity nature of $\ddot{u}\Lambda$ CDM gives the opportunity to avoid the cycle of positive correlation of A_L and H_0 and the negative correlation of A_L and Ω_m .

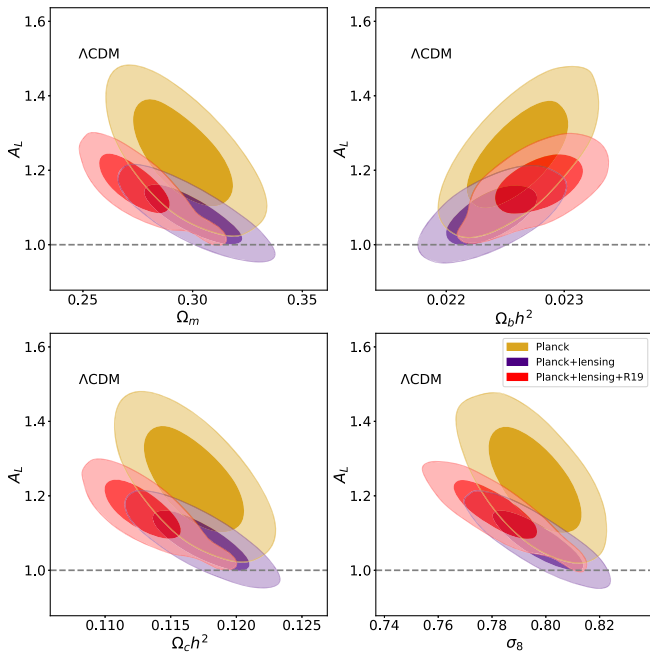


FIG. 5. The standard model's two-dimensional contour plots investigating the lensing amplitude versus matter density parameters of total matter, baryons, cold dark matter, and σ_8 are plotted.

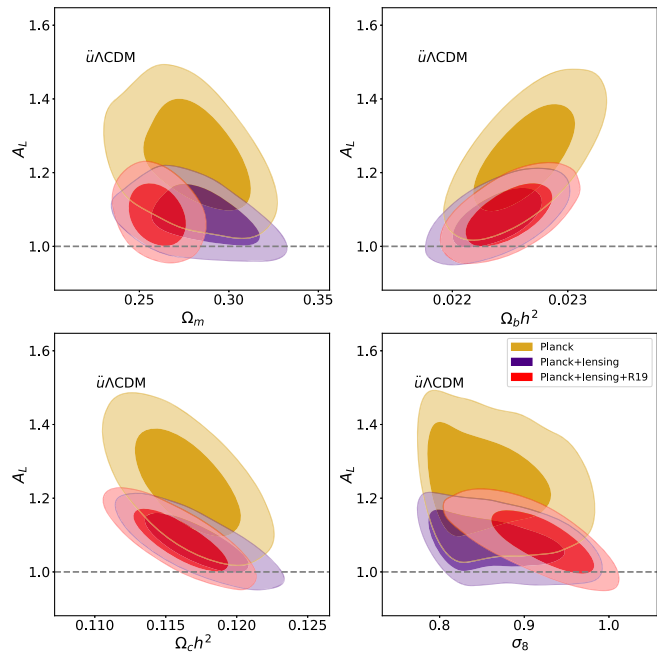


FIG. 6. Two-dimensional contour plots of $\ddot{u}\Lambda$ CDM, investigating the lensing amplitude versus matter density parameters of total matter, baryons, cold dark matter, and σ_8 , are plotted.

TABLE III. 68% C.L. constraints for the $\ddot{u}\Lambda$ CDM and Λ CDM models, for Planck, Planck + CMB lensing and Planck + CMB lensing + R19. Note that $a_{\oplus} = (1 + z_{\oplus})^{-1}$ and ν is degrees of freedom for χ^2 -test.

Parameters	Λ CDM	Λ CDM	Λ CDM	$\ddot{u}\Lambda$ CDM	$\ddot{u}\Lambda$ CDM	$\ddot{u}\Lambda$ CDM
	Planck	Planck + lensing	Planck + lensing + R19	Planck	Planck + lensing	Planck + lensing + R19
Ω_m	0.295 ± 0.015	$0.300^{+0.014}_{-0.015}$	$0.2744^{+0.0091}_{-0.012}$	$0.280^{+0.022}_{-0.017}$	$0.300^{+0.014}_{-0.015}$	$0.260^{+0.010}_{-0.011}$
H_0	68.9 ± 1.2	68.4 ± 1.1	$70.5^{+1.0}_{-0.85}$	$70.7^{+1.4}_{-2.6}$	$70.4^{+1.5}_{-2.6}$	73.2 ± 1.3
a_{\oplus}	>0.687	$0.75^{+0.13}_{-0.17}$	$0.607^{+0.031}_{-0.072}$
A_L	1.244 ± 0.095	1.081 ± 0.053	1.159 ± 0.056	1.244 ± 0.096	1.078 ± 0.053	1.087 ± 0.056
S_8	0.789 ± 0.030	0.797 ± 0.029	$0.748^{+0.020}_{-0.026}$	$0.826^{+0.038}_{-0.042}$	$0.838^{+0.039}_{-0.044}$	$0.854^{+0.041}_{-0.035}$
χ^2_{lensing}	...	$10.0(\nu:1.9)$	$9.98(\nu:2.3)$...	$9.9(\nu:2.0)$	$9.6(\nu:2.2)$
χ^2_{H074p03}	$6.5(\nu:7.7)$	$1.2(\nu:1.5)$
χ^2_{CMB}	$624.2(\nu:8.7)$	$637.7(\nu:7.0)$	$641.2(\nu:11.3)$	$624.1(\nu:7.3)$	$637.6(\nu:7.7)$	$637.9(\nu:8.0)$

In Fig. 5, we plot the two-dimensional contour plots of the standard model, investigating the lensing amplitude versus matter density parameters of total matter, baryons, cold dark matter, and σ_8 .

In Fig. 6, we plot the confidence level of $\ddot{u}\Lambda$ CDM for the lensing amplitude A_L versus matter density parameters of total matter, baryons, cold dark matter, and σ_8 . We find the anticipated correlations of A_L with the matter density. It is worth mentioning that $\ddot{u}\Lambda$ CDM shifts the σ_8 to the higher values, which will be a problem to compare this value with late-time observations. However, to further investigate this problem, we should look at the nonlinear structure formation in $\ddot{u}\Lambda$ CDM to compare it with cluster count and weak lensing data in a nonlinear regime. In Table III we summarize all the results. As we discussed in Sec. III, the ISW effect is the other secondary effect on CMB. We introduce the ISW to study the change of the gravitational potential in the dark energy-dominated era. In Fig. 7, we plot the ISW-galaxy cross-correlation function for both models of Λ CDM (black solid line) and $\ddot{u}\Lambda$ CDM (blue dashed line). We compare the models with the observational data of NVSS and WISE. We show that the $\ddot{u}\Lambda$ CDM is compatible with the ISW-galaxy cross-correlation data and it has an enhanced power in small angular scales due to

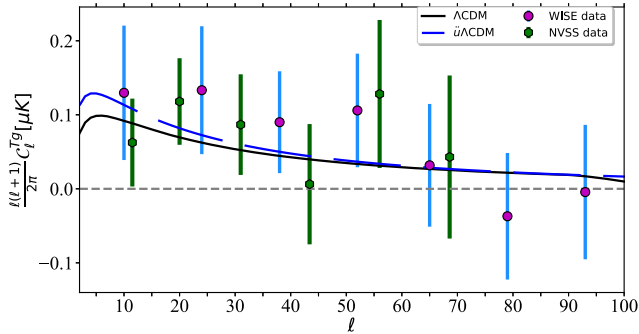


FIG. 7. The ISW-galaxy angular cross power spectrum is plotted for Λ CDM (black solid line) and $\ddot{u}\Lambda$ CDM (blue dashed line). The observational data are from the NVSS galaxy sample (hexagon points) and WISE (circle dots).

change of the gravitational potential in transition redshift. As a final word to this section, we should note that there are arguments in the literature on the validity of H_0 prior [53–55], as it is related to the absolute magnitude of SNe Ia and it is derived depending on the astrophysical model. This is not the essential concern in our work as we did not use SNe Ia data independently, which brings a twice usage of SNe Ia. Our transition in $\ddot{u}\Lambda$ CDM occurred at higher redshifts $z \sim 0.6$, which is out of the scope of the priors studied in [55]. However, in a series of works, it is shown that the simultaneous use of the BAO and SNe Ia data prevent the late-time models to solve the H_0 tension [54–58]. In our analysis, we did not use these two datasets, as we are focusing on the secondary gravitational effects on the CMB. So, we should be conservative in our assertion admitting that it is unlikely that $\ddot{u}\Lambda$ CDM can solve the H_0 tension fully once these additional datasets are used.

VI. CONCLUSION AND FUTURE REMARKS

In [37] we have shown $\ddot{u}\Lambda$ CDM can be a framework to study the H_0 tension. Here, we studied this model again to check if it can be a resolution for the CMB internal (mild) tensions. Interestingly, $\ddot{u}\Lambda$ CDM which is first proposed to address the H_0 tension can solve the CMB anomalies. Our model does not see any discrepancies between low- and high- ℓ 's power spectrum. The $\ddot{u}\Lambda$ CDM has no tension with $A_L = 1$ and R19 with just one additional free parameter in comparison to standard Λ CDM. The Λ CDM with A_L has an additional free parameter that can lessen H_0 tension but with a higher value for A_L . It means to address both H_0 and lensing tensions $\ddot{u}\Lambda$ CDM is as good as Λ CDM + A_L with the same number of free parameters. Physically, higher A_L means higher matter density, which is needed to solve the lensing anomaly. But in the $\ddot{u}\Lambda$ CDM model, higher lensing is not because of higher matter density, but because of the stronger gravity. This is the property in the heart of the construction of the $\ddot{u}\Lambda$ CDM, i.e., the way it is built. We also investigate the ISW effect via the cross-correlation with the galaxy distribution. We check the consistency of $\ddot{u}\Lambda$ CDM.

Finally, we should mention that stronger gravity may make the σ_8 tension worse. This issue needs more investigation in future works. Also, we should mention that as indicated beforehand as we did not use the SNe Ia and BAO, we should be conservative, indicating that it is unlikely that $\ddot{\Lambda}$ CDM can solve the H_0 tension fully once these additional datasets are used. Also, an investigation on the recently raised issue of the magnitude versus Hubble tension is needed to study in detail for models like $\ddot{\Lambda}$ CDM, which has a higher redshift transition. Another way to pursue this model is by looking at the nonlinear structure formation. On the theory side, it will be interesting to look at it, if we can model the perturbation of $\ddot{\Lambda}$ CDM differently.

ACKNOWLEDGMENTS

We thank the anonymous referee for his/her insightful comments and suggestion, which improved the manuscript extensively. N. K. and S. B. are in debt to the Abdus Salam International Center of Theoretical Physics (ICTP) for the very kind hospitality. The main part of the idea of this work has been developed there. S. B. is partially supported by Abdus Salam International Center of Theoretical Physics (ICTP) under the junior associateship scheme during this work. This research is supported by Sharif University of Technology Office of Vice President for Research under Grant No. G960202.

-
- [1] A. G. Riess *et al.*, A 2.4% determination of the local value of the Hubble constant, *Astrophys. J.* **826**, 56 (2016).
 - [2] A. G. Riess *et al.*, New parallaxes of galactic cepheids from spatially scanning the Hubble space telescope: Implications for the Hubble constant, *Astrophys. J.* **855**, 136 (2018).
 - [3] A. G. Riess, S. Casertano, W. Yuan, L. M. Macri, and D. Scolnic, Large magellanic cloud cepheid standards provide a 1% foundation for the determination of the Hubble constant and stronger evidence for physics beyond Λ CDM, *Astrophys. J.* **876**, 85 (2019).
 - [4] N. Aghanim *et al.* (Planck Collaboration), Planck 2018 results. VI. Cosmological parameters, *Astron. Astrophys.* **641**, A6 (2020).
 - [5] C. Heymans T. Tröster, M. Asgari, C. Blake, H. Hildebrandt, B. Joachimi, K. Kuijken, C. A. Lin, A. G. Sánchez, J. L. v. Busch *et al.*, KiDS-1000 Cosmology: Multiprobe weak gravitational lensing and spectroscopic galaxy clustering constraints, *Astron. Astrophys.* **646**, A140 (2021).
 - [6] S. Kumar and R. C. Nunes, Probing the interaction between dark matter and dark energy in the presence of massive neutrinos, *Phys. Rev. D* **94**, 123511 (2016).
 - [7] D. M. Xia and S. Wang, Constraining interacting dark energy models with latest cosmological observations, *Mon. Not. R. Astron. Soc.* **463**, 952 (2016).
 - [8] E. Di Valentino, A. Melchiorri, and O. Mena, Can interacting dark energy solve the H_0 tension?, *Phys. Rev. D* **96**, 043503 (2017).
 - [9] S. Kumar and R. C. Nunes, Echo of interactions in the dark sector, *Phys. Rev. D* **96**, 103511 (2017).
 - [10] A. Gómez-Valent, V. Pettorino, and L. Amendola, Update on coupled dark energy and the H_0 tension, *Phys. Rev. D* **101**, 123513 (2020).
 - [11] M. Lucca and D. C. Hooper, Tensions in the dark: Shedding light on dark matter–dark energy interactions, *Phys. Rev. D* **102**, 123502 (2020).
 - [12] C. Van De Bruck and J. Mifsud, Searching for dark matter–dark energy interactions: Going beyond the conformal case, *Phys. Rev. D* **97**, 023506 (2018).
 - [13] W. Yang, S. Pan, E. Di Valentino, R. C. Nunes, S. Vagnozzi, and D. F. Mota, Tale of stable interacting dark energy, observational signatures, and the H_0 tension, *J. Cosmol. Astropart. Phys.* **09** (2018) 019.
 - [14] W. Yang, A. Mukherjee, E. Di Valentino, and S. Pan, Interacting dark energy with time varying equation of state and the H_0 tension, *Phys. Rev. D* **98**, 123527 (2018).
 - [15] W. Yang, O. Mena, S. Pan, and E. Di Valentino, Dark sectors with dynamical coupling, *Phys. Rev. D* **100**, 083509 (2019).
 - [16] M. Martinelli, N. B. Hogg, S. Peirone, M. Bruni, and D. Wands, Constraints on the interacting vacuum–geodesic CDM scenario, *Mon. Not. R. Astron. Soc.* **488**, 3423 (2019).
 - [17] E. Di Valentino, A. Melchiorri, O. Mena, and S. Vagnozzi, Interacting dark energy in the early 2020s: A promising solution to the H_0 and cosmic shear tensions, *Phys. Dark Universe* **30**, 100666 (2020).
 - [18] E. Di Valentino, A. Melchiorri, O. Mena, and S. Vagnozzi, Nonminimal dark sector physics and cosmological tensions, *Phys. Rev. D* **101**, 063502 (2020).
 - [19] V. Pettorino, Testing modified gravity with Planck: The case of coupled dark energy, *Phys. Rev. D* **88**, 063519 (2013).
 - [20] W. Yang, E. Di Valentino, O. Mena, S. Pan, and R. C. Nunes, All-inclusive interacting dark sector cosmologies, *Phys. Rev. D* **101**, 083509 (2020).
 - [21] W. Yang, S. Pan, R. C. Nunes, and D. F. Mota, Dark calling dark: Interaction in the dark sector in presence of neutrino properties after Planck CMB final release, *J. Cosmol. Astropart. Phys.* **04** (2020) 008.
 - [22] W. Yang, S. Pan, L. Xu, and D. F. Mota, Effects of anisotropic stress in interacting dark matter–dark energy scenarios, *Mon. Not. R. Astron. Soc.* **482**, 1858 (2019).
 - [23] V. Poulin, T. L. Smith, T. Karwal, and M. Kamionkowski, Early Dark Energy Can Resolve The Hubble Tension, *Phys. Rev. Lett.* **122**, 221301 (2019).
 - [24] T. Karwal and M. Kamionkowski, Dark energy at early times, the Hubble parameter, and the string axiverse, *Phys. Rev. D* **94**, 103523 (2016).

- [25] V. Pettorino, L. Amendola, and C. Wetterich, How early is early dark energy?, *Phys. Rev. D* **87**, 083009 (2013).
- [26] A. Banihashemi, N. Khosravi, and A. H. Shirazi, Ginzburg-Landau theory of dark energy: A framework to study both temporal and spatial cosmological tensions simultaneously, *Phys. Rev. D* **99**, 083509 (2019).
- [27] A. Banihashemi, N. Khosravi, and A. H. Shirazi, Phase transition in the dark sector as a proposal to lessen cosmological tensions, *Phys. Rev. D* **101**, 123521 (2020).
- [28] M. Farhang and N. Khosravi, Phenomenological gravitational phase transition: Reconciliation between the late and early Universe, *Phys. Rev. D* **103**, 083523 (2021).
- [29] X. Li and A. Shafieloo, A simple phenomenological emergent dark energy model can resolve the Hubble tension, *Astrophys. J. Lett.* **883**, L3 (2019).
- [30] S. Pan, W. Yang, E. Di Valentino, A. Shafieloo, and S. Chakraborty, Reconciling H_0 tension in a six parameter space? *J. Cosmol. Astropart. Phys.* **06** (2020) 062.
- [31] X. Li and A. Shafieloo, Evidence for emergent dark energy, *Astrophys. J.* **902**, 58 (2020).
- [32] R. C. Nunes, Structure formation in $f(T)$ gravity and a solution for H_0 tension, *J. Cosmol. Astropart. Phys.* **05** (2018) 052.
- [33] M. Ballardini, M. Braglia, F. Finelli, D. Paoletti, A. A. Starobinsky, and C. Umiltà, Scalar-tensor theories of gravity, neutrino physics, and the H_0 tension, *J. Cosmol. Astropart. Phys.* **10** (2020) 044.
- [34] M. Braglia, M. Ballardini, F. Finelli, and K. Koyama, Early modified gravity in light of the H_0 tension and LSS data, *Phys. Rev. D* **103**, 043528 (2021).
- [35] N. Khosravi, Ensemble average theory of gravity, *Phys. Rev. D* **94**, 124035 (2016).
- [36] N. Khosravi, Über-gravity and the cosmological constant problem, *Phys. Dark Universe* **21**, 21 (2018).
- [37] N. Khosravi, S. Baghran, N. Afshordi, and N. Altamirano, H_0 tension as a hint for a transition in gravitational theory, *Phys. Rev. D* **99**, 103526 (2019).
- [38] F. Hassani, S. Baghran, and H. Firouzjahi, Lensing as a probe of early Universe: From CMB to galaxies, *J. Cosmol. Astropart. Phys.* **05** (2016) 044.
- [39] M. A. Fard and S. Baghran, Late time sky as a probe of steps and oscillations in primordial Universe, *J. Cosmol. Astropart. Phys.* **01** (2018) 051.
- [40] S. Baghran and S. Rahvar, Structure formation in $f(R)$ gravity: A distinguishing probe between the dark energy and modified gravity, *J. Cosmol. Astropart. Phys.* **12** (2010) 008.
- [41] A. Lewis and A. Challinor, Weak gravitational lensing of the CMB, *Phys. Rep.* **429**, 1 (2006).
- [42] N. Aghanim *et al.* (Planck Collaboration), Planck 2018 results. VIII. Gravitational lensing, *Astron. Astrophys.* **641**, A8 (2020).
- [43] F. Bianchini *et al.* (SPT Collaboration), Constraints on cosmological parameters from the 500 deg² SPTpol lensing power spectrum, *Astrophys. J.* **888**, 119 (2020).
- [44] L. Amendola and S. Tsujikawa, *Dark Energy: Theory and Observations* (Cambridge University Press, Cambridge, England, 2010).
- [45] S. Khosravi, A. Mollazadeh, and S. Baghran, ISW-galaxy cross correlation: A probe of dark energy clustering and distribution of dark matter tracers, *J. Cosmol. Astropart. Phys.* **09** (2016) 003.
- [46] N. Aghanim *et al.* (Planck Collaboration), Planck 2018 results. V. CMB power spectra and likelihoods, *Astron. Astrophys.* **641**, A5 (2020).
- [47] S. Ho, C. Hirata, N. Padmanabhan, U. Seljak, and N. Bahcall, Correlation of CMB with large-scale structure: I. ISW tomography and cosmological implications, *Phys. Rev. D* **78**, 043519 (2008).
- [48] E. L. Wright, P. R. M. Eisenhardt, A. Mainzer, M. E. Ressler, R. M. Cutri, T. Jarrett, J. D. Kirkpatrick, D. Padgett, R. S. McMillan, M. Skrutskie *et al.*, The wide-field infrared survey explorer (WISE): Mission description and initial on-orbit performance, *Astron. J.* **140**, 1868 (2010).
- [49] S. Ferraro, B. D. Sherwin, and D. N. Spergel, WISE measurement of the integrated Sachs-Wolfe effect, *Phys. Rev. D* **91**, 083533 (2015).
- [50] A. Hojjati, L. Pogosian, and G. B. Zhao, Testing gravity with CAMB and CosmoMC, *J. Cosmol. Astropart. Phys.* **08** (2011) 005.
- [51] A. Lewis and S. Bridle, Cosmological parameters from CMB and other data: A Monte Carlo approach, *Phys. Rev. D* **66**, 103511 (2002).
- [52] A. Gelman and D. B. Rubin, Inference from iterative simulation using multiple sequences, *Stat. Sci.* **7**, 457 (1992).
- [53] G. Benevento, W. Hu, and M. Raveri, Can late dark energy transitions raise the Hubble constant? *Phys. Rev. D* **101**, 103517 (2020).
- [54] D. Camarena and V. Marra, On the use of the local prior on the absolute magnitude of type Ia supernovae in cosmological inference, *Mon. Not. R. Astron. Soc.* **504**, 5164 (2021).
- [55] G. Efstathiou, To H_0 or not to H_0 ? [arXiv:2103.08723](https://arxiv.org/abs/2103.08723).
- [56] L. Perivolaropoulos and F. Skara, Challenges for Λ CDM: An update, [arXiv:2105.05208](https://arxiv.org/abs/2105.05208).
- [57] A. Banihashemi, N. Khosravi, and A. Shafieloo, Dark energy as a critical phenomenon: A hint from Hubble tension, *J. Cosmol. Astropart. Phys.* **06** (2021) 003.
- [58] R. G. Cai, Z. K. Guo, S. J. Wang, W. W. Yu, and Y. Zhou, A no-go guide for the Hubble tension, [arXiv:2107.13286](https://arxiv.org/abs/2107.13286).